A Study on Inter-vehicle Communication at 60GHz in NLOS Junction

#Atsuo KITANO [1], Toshitaka KOJIMA[2], Masaaki KOBAYASHI[3], Yiwei He[4]
[1]*Graduate School of Engineering, Kansai University*
3-3-35, Yamate-cho, Suita-shi, Osaka 564-8680, Japan
E-mail: kitano@optemlab.densi.kansai-u.ac.jp
[2]*Kansai University Frontier Science Center*
3-3-35, Yamate-cho, Suita-shi, Osaka 564-8680, Japan
E-mail: kojima@ipcku.kansai-u.ac.jp
[3]*Mitsubishi Electric Co.*
8-1-1, Tsukaguchihonmachi, Amagasaki-shi, Hyogo 661-8661, Japan
[4] *Osaka Electro-Communication University*
18-8, Hatsucho, Neyagawa-shi, Osaka 572-8680, Japan

Abstract

In recent year, the study of 60 GHz inter-vehicle communication (IVC) has been achieved mainly for line-of-sight (LOS) cases. However, much attention has not been paid to the IVC for the case of non line-of-sight (NLOS). Therefore, in this paper we try to examine the multipath propagation characteristics by taking the incoherent component in the NLOS case into consideration. Furthermore, this paper discusses the reception characteristics and the improvement effect by the use of adaptive array antenna (AAA) systems.

1. INTRODUCTION

Recently, the growth of the road traffic has given rise to serious road traffic problems such as traffic accident, congestion, and environmental pollution due to wasteful fuel consumption and a large amount of CO_2 exhaust.
As a powerful method for solving these problems, Intelligent Transport System (ITS) has been proposed. ITS is a new traffic system based on the share of the information among "Person", "Road", and "Vehicle" using a state-of-the-art information and communication technology (ICT) [1].
In ITS, the road-to-vehicle communication (RVC) system and the inter-vehicle communication (IVC) system have been proposed. As RVC system, Electronic Toll Collection system (ETC) and Vehicle Information and Communication System (VICS) have been realized so far. On the other hand, for the IVC system, the car communications system and the cooperation run system at road junction points are expected for safety road running. Moreover, IVC system can be utilized as the communication system for an emergency case where the existing communication system can not be used for the disaster such as earthquake, typhoon, and etc. However, for a realization of reliable IVC system, there exist a lot of problem to be solved, and it has not been put in practical use yet. In recent year, the study of millimeter-wave IVC has been done mainly for the line-of-sight (LOS) case. However, the non line-of-sight (NLOS) case has not been treated thoroughly.
In the present paper, therefore, we try to examine 60 GHz millimeter-wave propagation characteristics for a case of NLOS in IVC, by taking not only specularly but also nonspecularly reflected waves into account. Moreover, we also discuss the improvement of the reception characteristic by the use of the adaptive array antenna system.

2. ANALYSIS

An urban model for analysis is shown in Fig.1, which represents a typical T junction [2] where we will have a difficulty in IVC because LOS communication becomes impossible in a distance zone from the junction.
In this model, we assume that the roadway width is 3m, the shoulder width 1m, and the footway width 2m, respectively. Moreover, the road and the walls of the surrounding buildings are assumed to be asphalt and concrete [3], respectively. Various parameters and dimensions for the present model are shown in Table 1. The height of transmitting and receiving antennas is assumed to be 0.5m because they are installed in the bumper part.
In Fig.1, Lt is the distances between the transmitter and the stop lines of one lane at T junction and Lr between the receiver and the stop line on the other lane. In the present analysis, we assume that Lt takes three different values 10m, 20m, and 30m. Moreover, multiply reflected waves are considered for four times or less specularly and one time nonspecularly reflected waves. The diffraction effect is not taken into account. All reflecting planes are assumed to rough surfaces with standard deviation 1.0mm and rms slope 0.05. For the simulation of wave propagation, we use the ray tracing technique for specular components and the ray launching technique for diffused component, respectively.

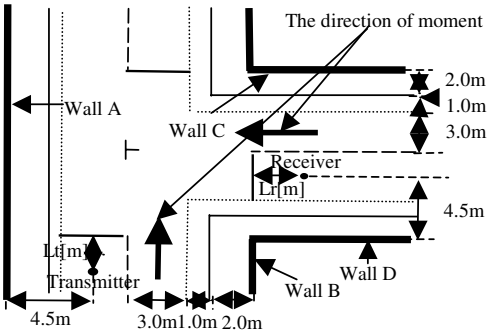

Fig.1: T junction model

TABLE 1: CONDITION FOR ANALYSIS.

Transmitter height	0.5 m
Receiver height	0.5 m
Frequency	60 GHz
Wavelength	5.0 mm
Direction of polarized wave	Vertically polarized wave
Atmosphere damping coefficient	15.09 dB/km
Complex index of refraction (asphalt)	2.00-j0.05
Complex index of refraction (concrete)	2.55-j0.14
Standard deviation (asphalt and concrete)	1.0 mm
RMS slope (asphalt and concrete)	0.05
Transmission power	10mW
Modulation system	BPSK
Noise temperature	300K
Band width	1MHz
Noise figure	10dB

We consider a vertically polarized case here.
The antenna system for the present analysis is shown in Fig. 2, where 7 microstrip antennas in vertical direction and 3 in horizontal one are located in an array plane with a period of half-wavelength. The directivities in vertical and horizontal planes are shown in Fig.3. Table 2 gives the specification of the array antenna.
The total directivity of the present antenna system is given by the product of the directivity of the antenna element and the array factor, that is, it can be expressed as follows[4],[5],[6]:

$$g(\theta,\phi) = \cos(\theta-\pi/2)\frac{\sin(kW\sin(\theta-\pi/2)/2)}{kW\sin(\theta-\pi/2)} \cdot \cos\left(\frac{kL}{2}\sin\left(\phi-\frac{\pi}{2}\right)\right)\cdot\left(\frac{1}{2}+\frac{1}{2}\cos u\right) \cdot\left(\frac{5}{16}+\frac{15}{32}\cos v+\frac{3}{16}\cos 2v+\frac{1}{32}\cos 3v\right) \quad (1)$$

where $u=\pi\sin(\phi-\pi/2), v=\pi\sin(\theta-\pi/2)$

and $L=W=\lambda/2\sqrt{\varepsilon_r}$.

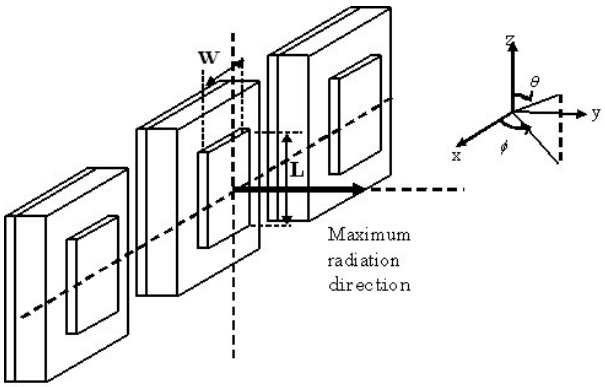

Fig.2: Microstrip array antenna.

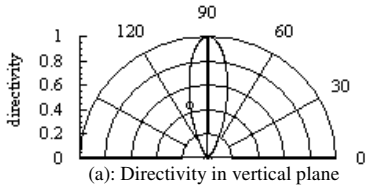

(a): Directivity in vertical plane

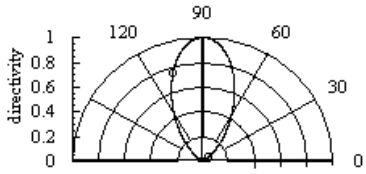

(b): Directivity in horizontal plane
Fig.3: Directivity of the antenna system.

TABLE 2 :PARAMETERS OF ARRAY ANTENNA.

Antenna element	Microstrip antenna
Dielectric constant	2.55
Element number	21 element
Array pattern	Binomial directivity
Transmission gain	16.22 dB

The gain of the antenna system is defined by

$$G(\theta,\phi) = 4\pi\frac{|g(\theta,\phi)|^2}{\int_0^{2\pi}\int_0^{\pi}|g(\theta,\phi)|^2\sin\theta d\phi d\theta} \quad (2)$$

Next, we consider both coherent and incoherent component waves between transmitting and receiving antennas. The coherent component consists of the direct wave and the specularly reflected waves. Considering the space attenuation term by Friis' transmission equation, the atmospheric attenuation term due to atmospheric absorption, and the reflection attenuation term by the Fresnel reflection coefficient, the total propagation loss L is given by

$$L = 20\log\left(\frac{\lambda}{4\pi d}\right)-\frac{\gamma d}{1000}+\sum 20\log(R) \quad (3)$$

where d is a propagation distance and R is a reflection coefficient. The ratio of received power to transmitted power P_{ratio} is expressed as follows:

$$P_{ratio} = 10\log\frac{P_R}{P_T} = 10\log G_T + 10\log G_R + L \qquad (4)$$

where G_T and G_R indicate the gains of the transmitter and the receiver, respectively.

In general, the specularly reflected component decreases due to the surface roughness of the reflection body. Therefore, the reflection coefficient R should be replaced by R', which is given by the following expression [7].

$$R' = R\exp\left(-2h_0^2 k^2 \cos^2\theta\right) \qquad (5)$$

In the above equation, R corresponds to the reflection coefficient without roughness and h_0 to the standard deviation of the height profile of the reflection surface. k is propagation vector $2\pi/\lambda$ in a free space, and θ is the angle of incidence.

The received power P_R due to nonspecularly reflected waves can be derived by the use of Beckmann's theory and the result is shown as following expression [8]:

$$P_R = \int_S \frac{P_T G_R G_T \lambda^2}{(4\pi)^3 r_1^2 r_2^2}\sigma_0 |R|^2 ds \qquad (6)$$

where r_1 and r_2 are the distances shown in Fig. 4, and R is the Fresnel reflection coefficients at the nonspecularly reflection point. The surface integral must be carried out on the surface S involving nonspecularly reflecting points under consideration. Moreover, σ_0 is given by the following expressions:

$$\sigma_0 = \begin{cases} \dfrac{\mu^4}{\beta_0^4}\sec^4\gamma\exp\left\{-\mu^2\left(1+\dfrac{\tan^2\gamma}{\beta_0^2}\right)\right\} & (\mu < 1) \\ \dfrac{1}{\beta_0^2}\sec^4\gamma\exp\left(-\dfrac{\tan^2\gamma}{\beta_0^2}\right) & (\mu \geq 1) \end{cases} \qquad (7)$$

where μ and γ are given by

$$\mu = h_0 k(\cos\theta_i + \cos\theta_s) \qquad (8)$$

$$\gamma = \tan^{-1}\frac{\sqrt{\cos^2\theta_i - 2\sin\theta_i\sin\theta_s\cos\psi_s + \cos^2\theta_s}}{\cos\theta_i + \cos\theta_s} \qquad (9)$$

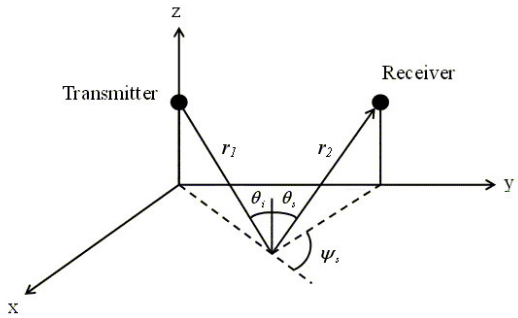

Fig.4 Propagation model for nonspecularly reflected waves.

β_0 is rms slope. θ_i,θ_s andψ_s are shown in Fig. 3.

Figure 5 shows a basic composition of N element AAA. Input signal vector X(t) to each antenna element and weight vector W to the signal are expressed as follows:

$$X(t) = [x_1(t), x_2(t), \cdots, x_N(t)]^T \qquad (10)$$

$$W = [w_1, w_2, \cdots, w_N]^T \qquad (11)$$

Superscript T denotes the transposition. The array output is given by

$$y(t) = W^H X(t) \qquad (12)$$

Superscript H indicates the complex conjugate transposition.

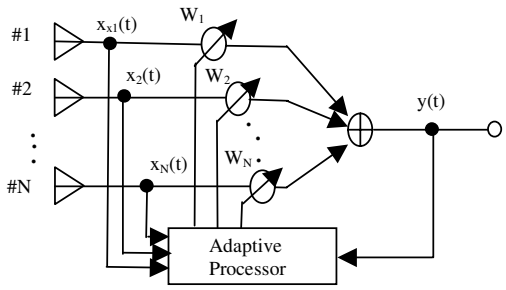

Fig.5: Composition of N element adaptive array.

In this analysis, Minimum Mean Square Error (MMSE) algorithm is used for obtaining optimum values of weights and Recursive Least-Squares (RLS) algorithm is used as an optimization technique of the MMSE algorithm. To minimize an error e(t) between the reference signal and the array out put, each weight W_i is updated in the RLS algorithm by the following recurrence formula [9], [10]:

$$W(m+1) = W(m) + \gamma R_{xx}^{-1}(m)X(m+1)e^*(m+1) \qquad (13)$$

$$\gamma = \frac{1}{\alpha + X^H(m+1)R_{xx}^{-1}(m)X(m+1)} \qquad (14)$$

$R_{xx}(m)$ denotes the correlation matrix of the reception signal, and α is a forgetting factor, and α=1 is assumed in this analysis. For the reference signal r(t), the error e(t) can be obtained as follows:

$$e(t) = r(t) - y(t) = r(t) - W^H X(t) \tag{15}$$

$R_{xx}(m)$ is renewed based on the next expressions.

$$\begin{cases} R_{xx}(0) = I \\ R_{xx}(m) = \alpha R_{xx}(m-1) + X(m)X^H(m) \end{cases} \tag{16}$$

where I is an unit matrix.

3. Results and Discussions

When the wave propagation path of coherent components that reaches the reception antenna in the urban model of Fig. 1 is simulated by using the ray tracing method, it is understood that there are 15 kinds of wave propagation paths as shown in Table 3 including the direct wave. In Table 3 and the following figures, "direct" stands for the case where the direct wave from transmitter is received, and "path1-1" , path1-2 , and "path1-3" do for the cases where the transmitted waves are received after they are specularly reflected by the ground, wall A ,and wall C, repectively.

Figs. 6-8 show the calculated results of P_{ratio} in Eq. (4) for coherent components along each path in the T junction model. Fig.6 corresponds to the case where the received wave is the direct one or specularly reflected only once, Fig.7 to the case where the received waves are specularly reflected twice, and Fig. 8 to the case reflected three or four times. From Fig. 6, it is shown that the direct wave can not be received at Lr=3m, 2m, 1m or more for Lt=10m, 20m, and 30m, respectively. Moreover, it is understood that the power ratio of each coming wave depends on the directivity of the antennas. For example, we can see that P_{ratio} is increased by the increase of the distance of the receiver Lr for the case of path1-3 and Lt=10m. This is because that the direction of the coming wave approaches the direction of maximum gain of antennas.

We can observe the similar tendency in Fig. 7 and Fig. 8.

From Figs. 7 and 8, we can see that it is hard to receive the coming wave in the range more than Lr=30m, 17m, and 10m for corresponding values of Lt.

An example of the simulated results of P_{ratio} for nonspecularly reflected waves is shown Fig. 9. In this result, we consider the received wave which arrives at the reception point after reflected nonspecularly only once by the ground, wall A or wall B. For reference, P_{ratio} for coherent components are calculated by synthesizing them under the consideration of their phases. Because the vertical directivity is sharper than that in horizontal one, P_{ratio} for road becomes smaller than that for wall A and wall B. Moreover, the power ratio of incoherent component for Lt is 10 and 20m becomes greater than that of coherent one by 10 dB or more in some ranges of Lr.

Fig. 10 shows the delay profile for Lr=1m. It is shown that the delay time of each arrival wave decreases because the difference between the propagation path lengths of the early coming wave and the delayed wave becomes small as the distance between the transmitter and receiver increases.

Table 3 : Path of Reflected Wave.

path1-1	ground
path1-2	wall A
path1-3	wall C
path2-1	wall A→ground
path2-2	ground→wall C
path2-3	wall B→wall A
path2-4	wall A→wall C
path2-5	wall C→wall D
path3-1	wall B→ground→wall A
path3-2	ground→wall A→wall C
path3-3	ground→wall C→wall D
path3-4	wall A→wall B→wall A
path4-1	wall A→wall B→ground→wall A
path4-2	wall B→wall A→wall B→wall A

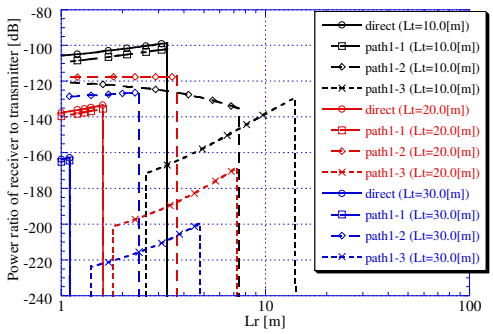

Fig.6: Distance characteristic of relative reception power of the coherent component (direct wave and one time reflected wave)

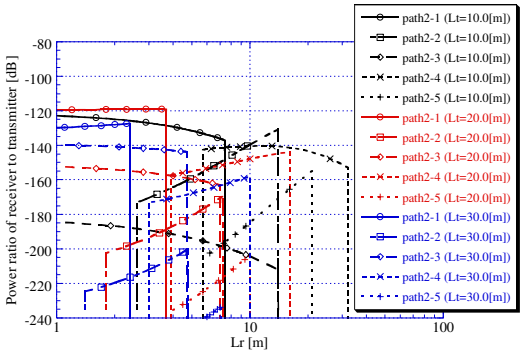

Fig.7: Distance characteristic of relative reception power of the coherent component (two times reflected wave).

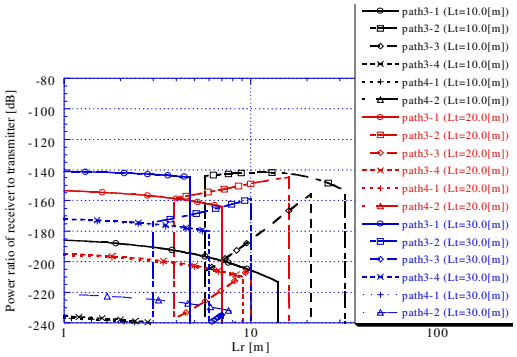

Fig.8: Distance characteristic of relative reception power of the coherent component (three and four times reflected waves).

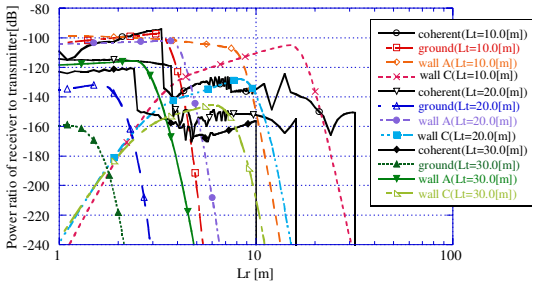

Fig.9: Distance characteristic of relative reception power of incoherent components.

Fig. 11 shows the total power ratio including both the coherent and incoherent components by considering their phases. For Lt=10, 20, and 30m, the relative received power is decreased greatly at about Lr=3.3, 3.7, and 2.4 m, because the maximum reflected wave can not arrive. However, the power is increased temporarily as the increase of Lr over those values, because the direction of coming waves approaches the direction of maximum gain of antennas and also the contribution from the incoherent waves is increased. Finally, the received power vanishes at Lr=32, 17, and 10m or more.

Fig. 12 shows the relation between Lr and bit error rate (BER) when the differential detection of binary phase shift keying (BPSK) is used. In this analysis, necessary BER is assumed to be 10^{-5}. From this figure, when the AAA (Correspond to BPSK in the figure) is not used, the rate of error is very high in all ranges of Lr for Lt=20m or more, and hence the detection of exact signals is difficult when only BPSK is used for such situations. For Lt=10m, good BER can be obtained in some ranges of Lr, however the steady detection of signal becomes difficult for almost all ranges of Lr.

On the other hand, when the AAA is used as an receiving antenna (AAA in the figure), BER becomes 10^{-5} or less in the rages less than Lr= 15 , 9, and 6m for each Lt. That is, the BER characteristic can be improved by the use of AAA.

However, in order to expand the range of Lr with good BER characteristics, some other efficient method should be required.

4. CONCLUSION

The millimeter-wave propagation in the T junction model has been analyzed and the effect of the improvement of the reception characteristic by the use of the AAA has been examined in this analysis. As the result, it has been shown that the distance for IVC can be expanded with the aid of the AAA. It will be necessary to examine the improvement of the distance by using the multi hop communication as a future problem.

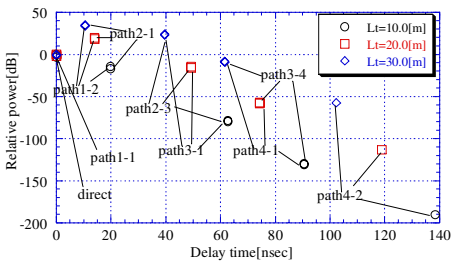

Fig.10: Delay profile characteristics.

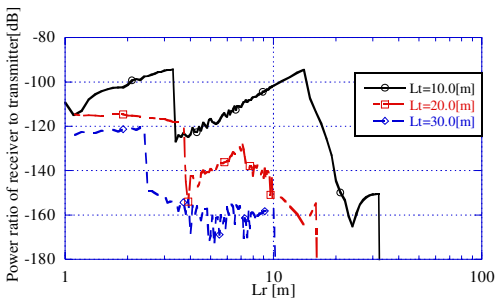

Fig.11: Distance characteristic of relative reception power.

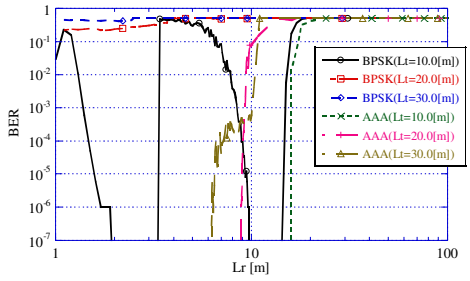

Fig.12: Relation between receiver position and BER.

ACKNOWLEDGMENT

This research work is supported by Kansai University Frontier Science Center, based on the partial support by the Ministry of Education, Culture, Sports, Science and Technology.

REFERENCES

[1] Japanese Ministry of Land, Infrastructure and Transport Road Bureau ITS homepage http://www.mlit.go.jp/road/ITS/j-html/.

[2] J. Maurer, T.M. Schafer, and W. Wansbeck, "A realistic description of the environment for inter-vehicle wave propagation modeling", IEEE Veh. Tech. Conf. VTC01-Fall, Atlantic City, NJ USA, Sep. 2001, vol. 3, pp. 1437-1441.

[3] K.Sato, T.Manabe, T.Ihara, Y.Kasashima, and K.Yamaki, "Measurements of Reflectivities of Interior Construction Materials at 60 GHz", IEICE Technical Report, AP 93-36, pp.1-7, June 1993.

[4] K.Fujimoto, Y.Yamada, and K.Tsunekawa, "An Illustrated Antenna System for Mobile Communication (in Japanese)", Sougoudennshishuppannsha, Tokyo, Oct.1996.

[5] N.Goto, "An Illustrated Antenna (in Japanese)", IEICE, Tokyo, Mar.1995.

[6] H.Arai, "New Antenna Engineering (in Japanese)", Sougoudennshishuppannsha, Tokyo, Apr.1996.

[7] P. Beckmann and A. Spizzichino, "The Scattering of Electromagnetic Waves form Rough Surfaces", Artech House Inc, 1987

[8] K.Tokuda, Y.Shiraki, K.Sekine, and S.Hoshina, "Analysis of Millimeter-Wave Band Road Surface Reflection Fading in Inter-Vehicle Communications", IEICE Technical Report, AP98-134, pp.27-34, Jan 1999.

[9] H.Sasaoka, "Mobile Communication (in Japanese)", Ohmsha, Tokyo, May 1998.

[10] Y.Kikuma, "Adaptive Antenna Technology (in Japanese)", Ohmsha, Tokyo, Oct 2003.